Effects of C–H stretch excitation on the H+CH_4 reaction

Jon P. Camden, Hans A. Bechtel, Davida J. Ankeny Brown, and Richard N. Zare[a)]
Department of Chemistry, Stanford University, Stanford, California 94305-5080

(Received 1 July 2005; accepted 20 July 2005; published online 30 September 2005)

We have investigated the effects of C–H stretching excitation on the H+$CH_4 \rightarrow CH_3+H_2$ reaction dynamics using the *photo-LOC* technique. The CH_3 product vibrational state and angular distribution are measured for the reaction of fast H atoms with methane excited in either the antisymmetric stretching fundamental ($\nu_3=1$) or first overtone ($\nu_3=2$) with a center-of-mass collision energy of E_{coll} ranging from 1.52 to 2.20 eV. We find that vibrational excitation of the $\nu_3=1$ mode enhances the overall reaction cross section by a factor of 3.0 ± 1.5 for $E_{coll}=1.52$ eV, and this enhancement factor is approximately constant over the 1.52–2.20-eV collision energy range. A local-mode description of the CH_4 stretching vibration, in which the C–H oscillators are uncoupled, is used to describe the observed state distributions. In this model, the interaction of the incident H atom with either a stretched or an unstretched C–H oscillator determines the vibrational state of the CH_3 product. We also compare these results to the similar quantities obtained previously for the Cl+$CH_4 \rightarrow CH_3$+HCl reaction at $E_{coll}=0.16$ eV [Z. H. Kim, H. A. Bechtel, and R. N. Zare, J. Chem. Phys. **117**, 3232 (2002); H. A. Bechtel, J. P. Camden, D. J. A. Brown, and R. N. Zare, *ibid.* **120**, 5096 (2004)] in an attempt to elucidate the differences in reactivity for the same initially prepared vibration. © *2005 American Institute of Physics*. [DOI: 10.1063/1.2034507]

I. INTRODUCTION

Knowledge of the role that molecular vibrations play in transforming reagents into products is essential to a fundamental understanding of chemical reactivity and of practical importance. For example, reactions of vibrationally excited species have been implicated in the "ozone deficit" problem,[1] have proved to be important when modeling high-temperature combustion chemistry,[2,3] and can influence the rate constants of chemical reactions.[4] Over the years, much progress has been made toward understanding the role of vibrations in chemical reactions. Polanyi[5] demonstrated that vibrational excitation is more effective at promoting reaction than an equivalent amount of enery in translation for late-barrier atom+diatom reactions. The larger number and variety of vibrational motions in polyatomic reagents, however, allow more complicated questions to be asked regarding the role of vibrational excitation in chemical reactions involving polyatomics.

A detailed experimental investigation of the role of vibrations in the H+$CH_4 \rightarrow CH_3+H_2$ reaction is appealing for several reasons. Besides playing an important role in hydrocarbon combustion chemistry,[6] the H+CH_4 reaction is the simplest reaction at a tetrahedrally bonded carbon atom. Having only five light atoms in addition to the carbon atom makes it amenable to high-level theoretical calculations. Consequently, it maintains as a prototypical polyatomic reaction and has become a testing ground for new theoretical methods.[7–10] In a pioneering study of the CH_5 system, Chapman and Bunker[11] explored the effect of vibrations on this system using quasiclassical trajectory (QCT) calculations in full dimensionality. They attempted to correlate features of the potential-energy surface to specific dynamical features. Although such generalizations proved difficult, they found that H_2 vibration enhanced the $CH_3+H_2 \rightarrow CH_4+H$ reaction, whereas CH_3 bending suppressed the reaction over a range of collision energies. Since this early work, theoretical studies employing quantum dynamics,[12–19] quasiclassical trajectory calculations,[20] and reaction-path analysis[21–23] all indicate that C–H stretch excitation enhances the H+CH_4 reaction rate. To date, however, no experimental verification exists of these predictions. Furthermore, while much effort has been directed at the kinetics[24–28] of the ground-state reaction, there have been only a few studies of the product-state-resolved dynamics[29,30] and none that prepare and detect a specific reactant and product quantum state.

Reactions of vibrationally excited methane are also of interest because methane serves as a prototypical polyatomic molecule. In addition, the infrared spectroscopy of methane is well characterized. Using laser-based techniques, it is possible to prepare well-defined vibrational eigenstates. The number of systems studied, however, still remains small. In a series of papers beginning in 1993, Zare and co-workers[31–42] studied the effects of fundamental, combination, and overtone band excitation of methane on the Cl+CH_4 reaction. Crim and co-workers[43–45] have also explored methane vibrational excitation in this reaction. Recently, the study of stretch-excited methane reactivity has been extended to Ni surfaces.[46–49] These studies have elucidated a wide range of phenomena that are attributed to the excitation of the methane reagent. For example, both mode selectivity, i.e., the mode of internal excitation controls the reaction outcome, and lack of mode selectivity have been observed. Dramatic bond selectivity for isotopomers of methane has also been

[a)]Author to whom correspondence should be addressed. Electronic mail: zare@stanford.edu

demonstrated. In some cases, reagent vibration is shown to be more effective than an equivalent amount of energy in translation.

In this paper, we report a study of the methyl radical product from the reactions:

$$H + CH_4(\nu_3 = 0) \rightarrow CH_3 + H_2, \tag{1a}$$

$$H + CH_4(\nu_3 = 1) \rightarrow CH_3 + H_2, \tag{1b}$$

$$H + CH_4(\nu_3 = 2) \rightarrow CH_3 + H_2. \tag{1c}$$

The focus of this work is twofold: (1) to explore the effect of reagent vibrational excitation on the reaction dynamics of this benchmark polyatomic system and (2) to make comparisons between the reactions of H and Cl atoms with stretch-excited methane. After a brief description of the background and experimental details, we discuss the CH_3 product-state and angular distributions that result from reactions (1a)–(1c). These quantities are compared to similar quantities obtained previously[38,40] for the reaction of Cl with $CH_4(\nu_3=0,1,2)$. We present a simple model that might explain the observed differences. Furthermore, we present the relative enhancement factor for the reaction $H+CH_4(\nu_3=1)\rightarrow CH_3(\nu=0)+H_2$ for collision energies between 1.52 and 2.20 eV.

II. BACKGROUND

A. Infrared spectroscopy of the ν_3 fundamental and $2\nu_3$ overtone

Methane belongs to the T_d point group and has four normal modes of vibration:[50] ν_1 (A_1, 2917 cm^{-1}, symmetric stretch), ν_2 (E, 1533 cm^{-1}, torsion), ν_3 (F_2, 3019 cm^{-1}, antisymmetric stretch), and ν_4 (F_2, 1311 cm^{-1}, bending). The ν_3 mode is triply degenerate and infrared active, whereas the $2\nu_3$ overtone is split into three sublevels, A_1, F_2, and E, of which only the $2\nu_3(F_2)$ sublevel is accessible by one-photon IR absorption. The C–H stretching modes also have a small bending mode character caused by a Fermi resonance between the stretching and bending vibrations in CH_4. Therefore, a more detailed treatment, which involves grouping vibrational levels into polyads,[51] is often used.

Nevertheless, theoretical models of the IR spectrum of CH_4 have demonstrated that a combination of local-mode stretching and harmonic bending mode basis functions provides an accurate description of the CH_4 overtone spectrum.[52] In the local-mode notation, ν_3 is denoted by $|1000,F_2\rangle$ and $2\nu_3(F_2)$ by $|1100,F_2\rangle$, where $|H_aH_bH_cH_d\rangle$ represents the number of quanta in the individual C–H oscillators. This analysis suggests that the ν_3 fundamental acts as if there is one quantum of vibration in one local C–H oscillator, whereas the $2\nu_3$ overtone acts as if there is one quantum in each of two C–H oscillators. We point out, however, that the overtone eigenstate contains about 10% bending mode character. While the local-mode description of the $\nu_3=1$ vibration may be less appropriate than the normal-mode picture, we will argue later that the local mode is more useful for understanding the reactivity of H and Cl atoms with stretch-excited methane.

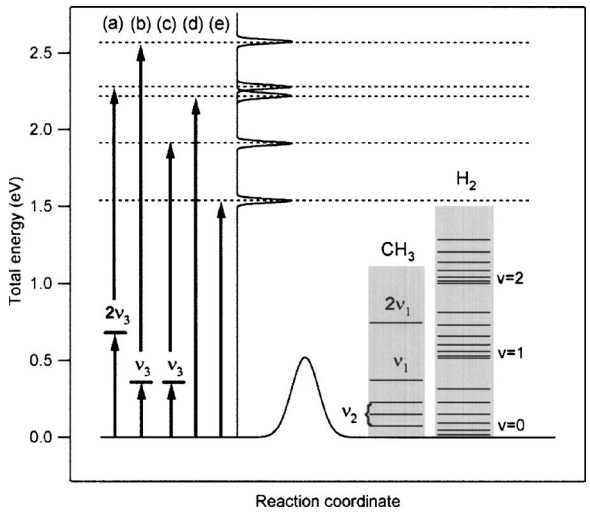

FIG. 1. Energetics for the $H+CH_4\rightarrow H_2+CH_3$ reaction. The total energy available for the reaction is given by the sum of the translational and vibrational energies, and the five different combinations probed in this work are described by Eqs. (2a)–(2e) in the text. The collision energy broadening is calculated by the formulas of van der Zande *et al.* (Ref. 68). Selected CH_3 and H_2 product-state energy levels are given on the right side.

B. Reaction energetics

The $H+CH_4\rightarrow CH_3+H_2$ reaction is nearly thermoneutral,[53] $\Delta H(0\ K)=9.3\times10^{-4}$ eV=8 cm^{-1}. High-level *ab initio* calculations,[23,54,55] the most recent of which have been corrected using the infinite basis-set extrapolation method of Fast *et al.*,[56] indicate a large classical barrier of 0.577 eV (4654 cm^{-1}). Photolysis of the HBr precursor at 230 or 202.5 nm provides a center-of-mass collision energy (E_{coll}) of 1.52 ± 0.05 or 2.20 ± 0.05 eV (12 260 or 17 740 cm^{-1}). Excitation of the C–H antisymmetric stretching fundamental ($\nu_3=1$) or overtone ($\nu_3=2$) can supply an additional 0.37 or 0.74 eV (3019 or 6005 cm^{-1}) of energy, respectively. Several different combinations of relative reagent translational (E_{coll}) and vibrational energy were used in the present study to overcome the reaction barrier:

$$H + CH_4(\nu_3 = 2), \quad E_{coll} = 1.52\ eV, \quad E_{tot} = 2.26\ eV, \tag{2a}$$

$$H + CH_4(\nu_3 = 1), \quad E_{coll} = 2.20\ eV, \quad E_{tot} = 2.57\ eV, \tag{2b}$$

$$H + CH_4(\nu_3 = 1), \quad E_{coll} = 1.52\ eV, \quad E_{tot} = 1.89\ eV, \tag{2c}$$

$$H + CH_4(\nu = 0), \quad E_{coll} = 2.20\ eV, \quad E_{tot} = 2.20\ eV, \tag{2d}$$

$$H + CH_4(\nu = 0), \quad E_{coll} = 1.52\ eV, \quad E_{tot} = 1.52\ eV. \tag{2e}$$

Therefore, this work presents an interesting opportunity to explore the effect of partitioning roughly the same total energy into different amounts of translation and vibration. Figure 1 illustrates these channels as well as the energies of

several H_2 (ω_e=4401 cm^{-1}, B_e=60.8 cm^{-1}) product quantum states and CH_3 vibrational levels [symmetric stretching (ν_1=3004 cm^{-1}), umbrella bending (ν_2=606 cm^{-1}), antisymmetric stretching (ν_3=3161 cm^{-1}), and deformation (ν_4=~1400 cm^{-1})].

III. EXPERIMENT

The current experimental apparatus and the application of core-extraction time-of-flight mass spectrometry to obtain laboratory-frame speed distributions have been described in detail elsewhere;[32] therefore, only the primary features are described here. Hydrogen bromide (Matheson, 99.999%), methane (Matheson, research grade, 99.999%), and helium (Liquid Carbonic, 99.995%) are mixed in a glass bulb and delivered to a pulsed supersonic nozzle (General Valve, Series 9, 0.6-mm orifice, backing pressure ~700 torr). The resulting molecular beam enters the extraction region of a Wiley-McLaren time-of flight (TOF) spectrometer where it is intersected by three laser beams that prepare the reagent quantum state, initiate the reaction, and state selectively probe the products.

The methane antisymmetric stretching fundamental or overtone is prepared by direct infrared absorption around 3.3 or 1.7 μm, respectively, and fast H atoms are generated by the UV (200–230 nm) photolysis of HBr. After a time delay of 20–30 ns, the nascent CH_3 reaction products are state selectively ionized using a 2+1 resonance-enhanced multiphoton ionization (REMPI) scheme via the $3p_z\ ^2A_2'' \leftarrow X\ ^2A_2''$ transition.[57] In order to ensure that the measurements were not biased by faster moving products flying out of the probe volume before the slower moving ones, all measurements were made at a time delay for which the CH_3 product signal was a linear function of the time delay. The product ions separate according to their mass and are detected by microchannel plates. Because the reactions of H atoms with both ground-state methane and vibrationally excited methane can produce CH_3, the IR light is modulated on and off on a shot-by-shot basis and the signal is recorded when the IR laser is on, S_{on}, and off, S_{off}. We refer to the signal obtained without the IR laser, S_{off}, as the ground-state reaction because it originates from methane molecules in their ground vibrational state. The subtraction S_{on}-S_{off} results in a difference signal, which is a measure of the enhancement (positive) or suppresion (negative) arising from vibrational excitation of the CH_4 reagent.

Excitation of ν_3=1 requires light around 3.3 μm, whereas ν_3=2 requires light around 1.7 μm. Tunable infrared light around 1.7 μm is generated by mixing the visible output of a Nd^{3+}:yttrium aluminum garnet (YAG) (Continuum PL9020) pumped dye laser (Continuum, ND6000; Exciton, DCM) with the 1.064-μm YAG fundamental in a beta-barium borate (BBO) crystal. The 1.7-μm light is then parametrically amplified in a $LiNbO_3$ crystal which is pumped by 1.064-μm radiation. Using this scheme, we obtained ~20 mJ after the difference frequency stage and ~55 mJ after amplification. The same scheme was used to obtain 3.3-μm light; however, instead of using the signal from the $LiNbO_3$ optical parametric amplification stage, the 3.3-μm idler (~10 mJ) was used. The 200–230-nm light was generated by frequency tripling in two BBO crystals the output of a Nd^{3+}:YAG (Continuum PL8020) pumped dye laser (Spectra Physics, PDL3; Exciton, Sulforhodamine 640 and LDS 698). The ~330-nm REMPI probe light was generated by frequency doubling in a BBO crystal the output of a Nd^{3+}:YAG (Spectra Physics DCR-2A) pumped dye laser (Lambda Physik, FL2002; Exciton, DCM/LDS698 mix).

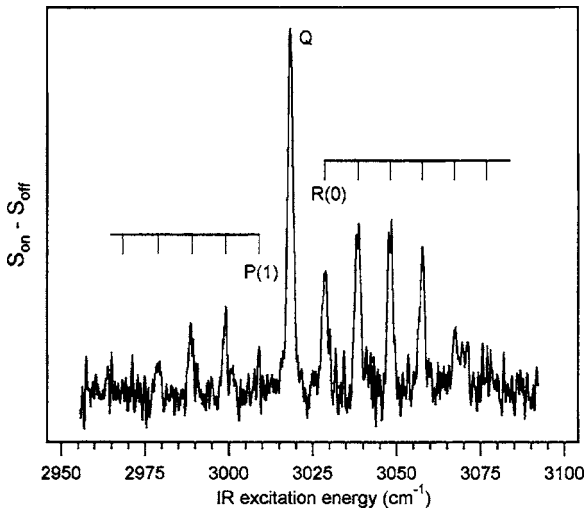

FIG. 2. Action spectrum recorded while monitoring the stretch-excited CH_3 from the H+CH_4(ν_3=1) reaction at E_{coll}=1.52 eV while the IR laser is scanned over the CH_4 ν_3 absorption feature indicating that the observed enhancement arises from methane vibration. The line positions of the *P*, *Q*, and *R* branches are obtained from the HITRAN database (Ref. 69).

The TOF mass spectrometer is operated in one of two modes. In the "crushed" mode, large extraction fields are used to collect all ions of a given mass that are formed in the focal volume of the probing laser. This mode is used to collect the REMPI spectra of the nascent methyl radical reaction products. In the "velocity-sensitive" mode, Wiley-McLaren space focusing conditions and lower extraction voltages are used to allow the m/z=15(CH_3^+) ions to separate according to their initial velocity. Furthermore, a core extractor is used to reject ions with velocities perpendicular to the flight tube axis, thus simplifying the data analysis. A Monte Carlo simulation is employed to generate an instrument response function for ions of a given initial laboratory-frame speed. The entire product speed range can be covered using these basis functions, which allows the measured TOF profile to be converted into a laboratory-frame speed distribution.

IV. RESULTS

A. Evidence of ν_3 reactivity and vibrational state distributions of the CH_3 products

Figure 2 presents the action spectrum of the H+CH_4(ν_3=1)→CH_3(ν_1=1) reaction for E_{coll}=1.52 eV obtained by monitoring the 1_1^1 vibrational hot band of the CH_3 $3p_z\ ^2A_2'' \leftarrow X\ ^2A_2''$ 2+1 REMPI transition while scanning the IR laser over the CH_4(ν_3) absorption feature. The spectrum is obtained by recording the difference of the m/z=15 ion current when the IR laser is on and off. Methane is a symmetric top molecule and for the $F_2 \leftarrow A_1$ transition a

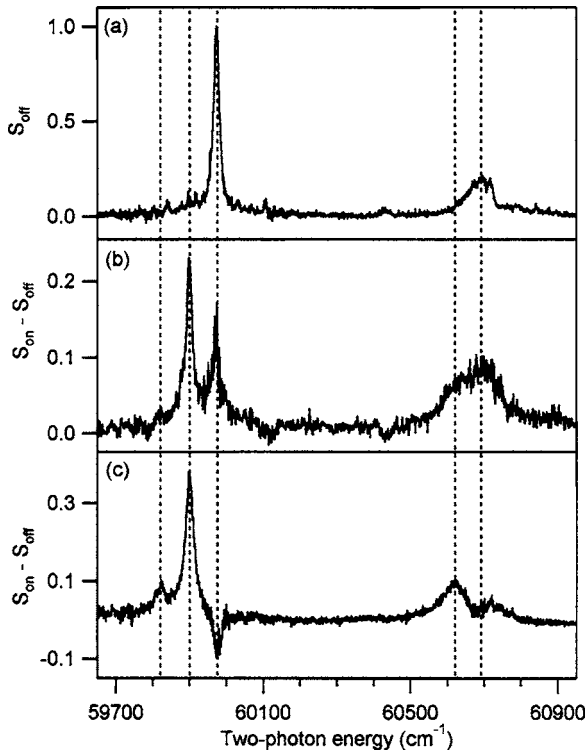

FIG. 3. Product $CH_3(2+1)3p_z \leftarrow X$ REMPI spectra for the reactions: (a) H $+CH_4(\nu=0)$, (b) $H+CH_4(\nu_3=1)$, and (c) $H+CH_4(\nu_3=2)$ for a center-of-mass collision energy $E_{coll}=1.52\pm0.05$ eV. From the left the positions of the 1_2^2 (C–H stretch overtone), 1_1^1 (C–H stretch), 0_0^0 (ground state), $1_1^1 2_1^1$ (symmetric stretching and umbrella bending combination), and 2_1^1 (umbrella bending mode) bands are marked by the vertical dotted lines. The signal when the IR laser is off (S_{off}) is the ground-state signal and (b) is the difference $S_{on}-S_{off}$ obtained while the IR laser pumps the $\nu_3=1$, $F_2 \leftarrow A_1$, Q branch while (c) is the difference $S_{on}-S_{off}$ obtained while the IR laser pumps the $\nu_3=2$, $F_2 \leftarrow A_1$, Q branch.

simple P, Q, and R branch structure is expected if Coriolis coupling is neglected.[50] Indeed, this behavior is observed for the ν_3 absorption band of methane and is reproduced well in the action spectrum of Fig. 2. Consequently, we can attribute the observed reactivity enhancement to the excitation of the ν_3 mode.

Figures 3 and 4 present the CH_3 REMPI spectra obtained for the reactions $H+CH_4(\nu)$ at two different collision energies: $E_{coll}=1.52$ eV and $E_{coll}=2.20$ eV, respectively. Figures 3(a) and 4(a) display the signal when the IR laser is off (S_{off}); Figs. 3(b) and 4(b) show the difference signal ($S_{on}-S_{off}$) obtained while the IR laser pumps the $\nu_3=1$, $F_2 \leftarrow A_1$, Q branch; and Fig. 3(c) shows the difference signal, $S_{on}-S_{off}$, obtained while pumping the $\nu_3=2$, $F_2 \leftarrow A_1$, Q branch. It is difficult to quantify rovibrational state distributions from the CH_3 REMPI spectra because one must consider the Franck-Condon factors for different vibrational bands and account for the rovibrational state-dependent predissociation of the upper electronic state.[57–59] Because of these difficulties and the modest signal-to-noise ratio of the current experiments, we do not extract detailed state distributions. All spectra, however, were obtained under the same experimental conditions, so we believe that comparisons between them are meaningful.

The REMPI spectra resulting from the ground-state reactions [Figs. 3(a) and 4(a)] at $E_{coll}=1.52$ eV and $E_{coll}=2.20$ eV, respectively, are dominated by the 0_0^0 Q-branch members and the smaller 2_1^1 band, indicating that mainly ground-state and methyl radicals excited in the umbrella bending mode are produced. This result is in good agreement with our previous work on the related $H+CD_4 \rightarrow CD_3+HD$ reaction[30] at a similar collision energy ($E_{coll}=1.95$ eV). The REMPI spectra of the vibrationally excited reactions [Figs. 3(b), 3(c), and 4(b)], however, show new features that cannot be attributed to ground-state or umbrella bending products. In particular, the spectra from both reactions have features assigned to the 1_1^1 band, indicating that the methyl radicals are produced with one quantum of symmetric-stretch vibrational excitation. The spectrum from the $H+CH_4(\nu_3=2)$ reaction also has features assigned to the 1_2^2 band (two quanta of symmetric stretching) and the $1_1^1 2_1^1$ combination band[60] (one quantum each of symmetric stretching and umbrella bending). These results clearly demonstrate that vibrational excitation has a significant impact on the product-state distributions of the $H+CH_4$ reaction.

Figure 3(c) has an additional feature worth noting: the difference signal is negative in the 0_0^0 Q-branch region of the spectrum, which means that the cross section for $CH_3(\nu=0)$ product formation is smaller for the vibrationally excited reaction than for the ground-state reaction. This result demonstrates how excitation of a vibrational mode, while putting more energy into the system, can actually decrease the cross section into a particular quantum state. We point out that for all other observed states there is an enhancement.

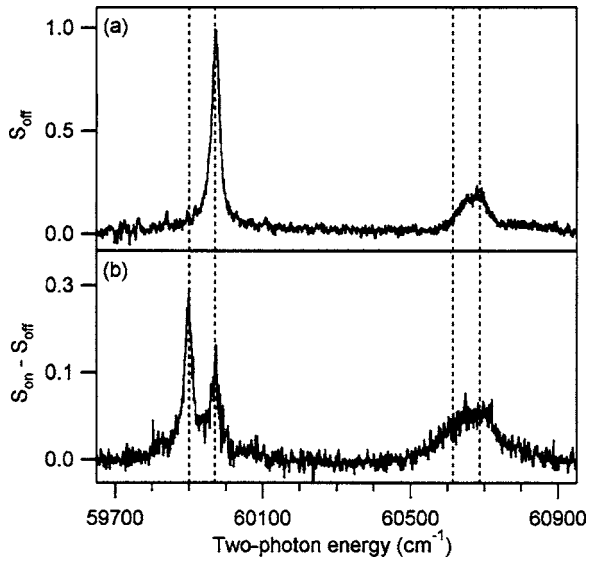

FIG. 4. Product $CH_3(2+1)3p_z \leftarrow X$ REMPI spectra for the reactions: (a) H $+CH_4(\nu=0)$ and (b) $H+CH_4(\nu_3=1)$ for a center-of-mass collision energy $E_{coll}=2.20\pm0.05$ eV. Reading from left to right, the positions of the 1_1^1 (C–H stretch), 0_0^0 (ground state), $1_1^1 2_1^1$ (symmetric stretching and umbrella bending combination), and 2_1^1 (umbrella bending mode) bands are marked by the vertical dotted lines. The signal when the IR laser is off (S_{off}) is the ground-state signal and (b) is the difference $S_{on}-S_{off}$ obtained while the IR laser pumps the $\nu_3=1$, $F_2 \leftarrow A_1$, Q branch. Within the experimental uncertainty no difference is observed between the spectra recorded at $E_{coll}=2.20$ eV and those obtained at $E_{coll}=1.52$ eV (Fig. 3).

B. Determination of the $\nu_3=1$ vibrational enhancement

S_{on} and S_{off} can be related to the reaction cross sections:

$$S_{off} \propto \sigma_{\nu=0}, \tag{3}$$

$$S_{on} \propto (1-x)\sigma_{\nu=0} + x\sigma_{\nu_3=1}, \tag{4}$$

where $\sigma_{\nu=0}$ is the cross section of the ground-state reaction, $\sigma_{\nu_3=1}$ is the cross section of the vibrationally excited reaction, and x is the fraction of methane molecules in the beam that are pumped to the excited state. Using these relations, the ratio of the vibrationally excited reaction cross section to that of the ground-state reaction cross section can be obtained:

$$\frac{\sigma_{\nu_3=1}}{\sigma_{\nu=0}} = \frac{(S_{on}/S_{off}-1)}{x} + 1. \tag{5}$$

In the current experiments S_{on} and S_{off} are recorded on an every other laser shot basis, making a determination of the ratio S_{on}/S_{off} straightforward. Furthermore, saturation of the one-photon IR transition constrains x to be less than 0.5 and allows for a calculation of the minimum enhancement. By integrating the area under the 0_0^0 band Q-branch members we determine the state-to-state specific enhancement factor F at a relative translational energy of 1.52 eV to be

$$F = \frac{\sigma[H + CH_4(\nu_3=1) \rightarrow CH_3(\nu=0) + H_2]}{\sigma[H + CH_4(\nu=0) \rightarrow CH_3(\nu=0) + H_2]} \geqslant 1.4. \tag{6}$$

The minimum enhancement for umbrella bending excited products is not reported because determination of this value is complicated by the presence of the $1_1^1 2_1^1$ combination band.

In order to make an estimate of the ratio of the total reaction cross sections, i.e., σ_{IR}/σ_{gs}, we make several approximations, which are important for future interpretation of these results. First, the bandwidth of the IR laser is not sufficient to overlap all rotational states in the molecular beam and some transitions may be only partially saturated, thus we believe a more reasonable estimate for x is $0.2 < x < 0.4$. Furthermore, while the minimum enhancement above was calculated only for reaction into the $CH_3(\nu=0)$ product state, we observe an enhancement for all of the states populated by the ground-state reaction. In addition, the H+$CH_4(\nu_3=1)$ reaction produces a significant amount of $CH_3(\nu_1=1)$. Because of the unknown Franck-Condon factors and predissociation rates of the $3p_z$ CH_3 Rydberg state, it is difficult to make an exact calculation of the population in this state. However, the sensitivity factor is not expected to be an order of magnitude different from that of the 0_0^0 band. Taking into account these factors we estimate that the total enhancement into all product states for $E_{coll}=1.52$ eV is

$$\frac{\sigma[H + CH_4(\nu_3=1)]}{\sigma[H + CH_4(\nu=0)]} = 3.0 \pm 1.5. \tag{7}$$

We have also measured the state-to-state relative enhancement factor [Eq. (6)] for the H+$CH_4(\nu_3=1) \rightarrow CH_3(\nu=0)$+$H_2$ product channel over the range of collision energies from 1.52 to 2.20 eV. The results, displayed in Fig. 5, indicate that within our uncertainty the enhancement remains constant. Here, we present the relative enhancement because our determination of the enhancement relative to other energies has a smaller uncertainty than that of the absolute enhancement. Lastly, our measurements of the CH_3 product-state distributions for the H+$CH_4(\nu_3=1)$ reaction are indistinguishable at $E_{coll}=1.52$ and 2.20 eV. Thus, a combination of Fig. 5 and Eq. (7) yields an enhancement of $\sigma_{IR}/\sigma_{gs}=3.0\pm1.5$ over the collision energy range of 1.52–2.20 eV. In principle, the same arguments should make a determination of the enhancement factor for the H+$CH_4(\nu_3=2)$ reaction possible; however, in practice it is more difficult to saturate the one-photon overtone transition and, thus, there is considerably more error in the value of x.

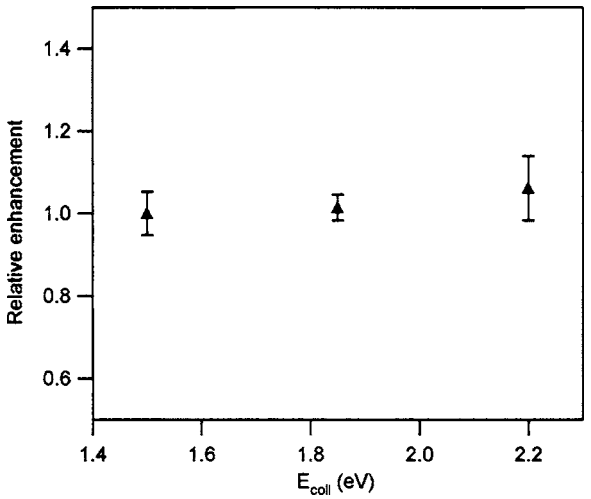

FIG. 5. Relative enhancement, $c(\sigma_{\nu_3=1}/\sigma_{\nu=0})$, for the reaction H+$CH_4(\nu_3=1) \rightarrow CH_3(\nu=0)$ channel as a function of the center-of-mass collision energy (E_{coll}). The constant c is chosen such that the enhancement factor $c(\sigma_{\nu_3=1}/\sigma_{\nu=0})=1$ for $E_{coll}=1.52$ eV. The uncertainty given is the statistical 95% confidence interval from replicate measurements.

C. Scattering distributions of the CH_3 products

Figure 6 shows the core-extracted isotropic and anisotropic TOF profiles obtained for the main product channels of each reaction studied:

$$H + CH_4(\nu=0) \rightarrow CH_3(\nu=0) + H_2, \tag{8a}$$

$$H + CH_4(\nu_3=1) \rightarrow CH_3(\nu_1=1) + H_2, \tag{8b}$$

$$H + CH_4(\nu_3=2) \rightarrow CH_3(\nu_1=1) + H_2, \tag{8c}$$

at a collision energy of 1.52 eV. The TOF profiles are then converted to the laboratory-frame speed distribution for each product channel. In a typical *photo-LOC* experiment the laboratory-frame speed is given by

$$v_{lab}^2 = u_{com}^2 + u_{prod}^2 + u_{com}u_{prod}\cos\theta, \tag{9}$$

where u_{com} is the speed of the center of mass, u_{prod} is the speed of the product CH_3 in the center-of-mass frame, and θ is the scattering angle with $\theta=0$ being forward scattered with respect to the incident H-atom direction.

Although the three reactions have different energetics, all three reaction channels yield the same laboratory-frame speed distribution within their uncertainties. For channels

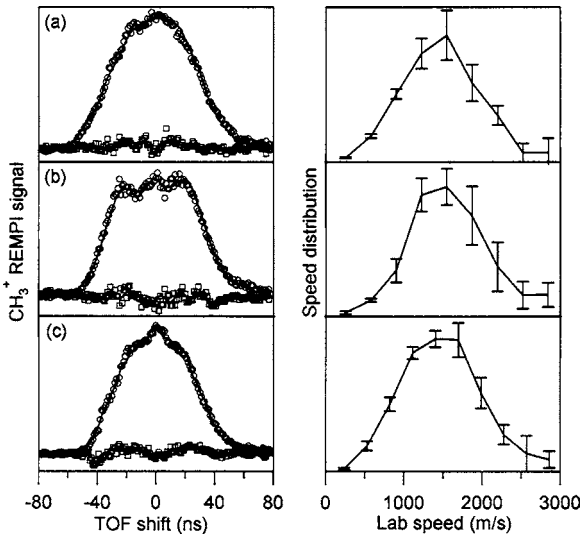

FIG. 6. Isotropic (○) and anisotropic (□) TOF profiles (left panel) and laboratory-frame speed distributions (right panel) of the state-to-state selected CH_3 products for (a) $H+CH_4(\nu=0)\rightarrow CH_3(\nu=0)+H_2$ observed on the $(2+1)3p_z-X\,0_0^0$ band Q branch, (b) $H+CH_4(\nu_3=1)\rightarrow CH_3(\nu_1=1)+H_2$, and (c) $H+CH_4(\nu_3=2)\rightarrow CH_3(\nu_1=1)+H_2$ observed on the $(2+1)3p_z-X\,1_1^1$ band Q branch. The uncertainty given is one standard deviation of replicate measurements and within this uncertainty the measured distributions are the indistinguishable.

(8a) and (8b), the CH_3 and H_2 products have nearly the same available energy because the energy of the $CH_4(\nu_3)$ and $CH_3(\nu_1)$ vibrations are very similar. The anisotropic component of the TOF profile is related to the average internal energy of the unobserved H_2 coproduct[38] and is the same for (8a) and (8b) within our confidence limits. Thus, we have reason to believe that the internal energy of the H_2 product is not significantly different for the two channels. From these observations, we conclude that the scattering dynamics for the reaction $H+CH_4(\nu=0)\rightarrow CH_3(\nu=0)+H_2$ and $H+CH_4(\nu_3=1)\rightarrow CH_3(\nu_1=1)+H_2$ channels are very similar, which indicates that the vibration remains a spectator. Reaction (8c), on the other hand, has an additional 3000 cm^{-1} more available to the CH_3 and H_2 products than reactions (8a) and (8b). Because the speed distribution is similar to that of (8a) and (8b), we conclude that either the products shift slightly more toward backward scattering, thus reducing the value of $\cos\theta$ in Eq. (9), or more energy is deposited into rotation and vibration of the H_2 coproduct, thus reducing u_{prod}. While subtle differences are possible, the overall trend for the ground-state and vibrationally excited reactions, (8a)–(8c), is the same: the CH_3 products scatter in the sideways and backward directions. A study of the $H+CH_4(\nu_3=1)\rightarrow CH_3(\nu=0)+H_2$ channel would also be interesting; however, interference from the ground-state reaction signal and limited signal-to-noise ratio make obtaining a reliable TOF profile difficult.

V. DISCUSSION

On energetic grounds alone, one might not expect vibrational excitation to be important in the $H+CH_4$ reaction at the high collisional energies employed here because the fraction of the total energy in vibration is small and in both cases the translational energy is much larger than the reaction barrier. However, as shown in Figs. 2–4, the $H+CH_4$ reaction is enhanced by excitation of the CH_4 antisymmetric stretching fundamental and overtone. We estimate that $\sigma_{\mathrm{IR}}/\sigma_{\mathrm{gs}}=3.0\pm1.5$ for ν_3 excited methane and that the ratio is the same for collision energies between 1.52 and 2.20 eV. We have recently measured[61] the relative excitation function for the related reaction $H+CD_4$ with collision energies between 1.48 and 2.36 eV finding that the cross section decreases by about a factor of 2 over this range. Thus, it is clear that vibrational excitation is much more effective than an equivalent amount of translational energy in promoting this reaction for the energies considered.

We also find that this reaction demonstrates striking mode selectivity. The vibrational state distributions from the reactions $H+CH_4(\nu_3=1)$ at 1.52 and 2.20 eV are the same within their uncertainty, but markedly different than the ground-state reaction indicating that the initially prepared vibration, not the translational energy, controls the product-state distribution. Furthermore, the reaction $H+CH_4(\nu_3=2)$ with $E_t=1.52$ eV has roughly the same total energy as the $H+CH_4(\nu=0)$ reaction with $E_t=2.20$ eV but they have dramatically different product distributions further illustrating that the increased energy available is not responsible for the change but rather it is the methane vibration.

A. The methane vibration acts as a local-mode C–H oscillator

A consideration of the transition state yields insight into the increased reactivity. In a simple picture, excitation of a reactant internal mode that is stretched in the transition state is expected to enhance the reaction. *Ab initio* calculations[23,54,55,62] of the abstraction transition state indicate that the geometry is more similar to the products than the reactants, i.e., the reaction has a late barrier. The nonreactive C–H bond lengths change little among the reactant CH_4 (1.091 Å), the C_{3v} saddle point (1.080 Å), and the product CH_3 (1.079 Å) suggesting that localization of the vibration into these bonds will have little effect on the reaction. The reactive C–H bond, however, is stretched significantly (1.400 Å) at the transition state. Thus, localization of the vibrational motion into this bond should enhance the reaction. In the local-mode picture of the CH_4 ν_3 vibration one of the four C–H bonds is locally excited while the others are not. Therefore, if the incoming H atom attacks a vibrationally excited C–H oscillator, the probability of reaction is expected to increase. Indeed, the vibrational state distributions support this picture. Furthermore, they suggest that the energy localized in the reactive bond is transferred to either the bending mode (ν_2) of the methyl radical product or into the H_2 product. In the case that the H atom is incident on a vibrationally unexcited C–H bond, the vibration present in the CH_4 reagent acts as a spectator playing no part in the reaction and leaving the methyl product with one quantum of C–H stretching. Although it is somewhat counterintuitive to think of the stretching fundamental in methane as a local mode, we believe it to be a better model to describe the reaction dynamics.

The above picture is easily generalized to account for the results obtained for the reactions of H with overtone-excited methane when one describes the $2\nu_3$ vibration in the local-mode basis set as $|1100,F_2\rangle$. The incoming H atom again is either incident on a locally stretched or unstretched C–H oscillator. If the H abstracts a stretched C–H bond, then the vibrational energy contained in the reactive bond is channeled into either the H_2 fragment or the CH_3 bending motion. However, because two local oscillators are initially excited, the CH_3 fragment is left with either one quantum of C–H stretching or in the stretching bending combination band. In the case the H atom reacts with an unstretched C–H bond the initially prepared CH_4 vibration remains a spectator and the CH_3 fragment contains two quanta of vibrational stretching excitation. Lastly, the H atom is unable to extract efficiently the vibrational energy from two local C–H oscillators. Indeed, we observe that the cross section to produce $CH_3(\nu=0)$ products is actually smaller for $CH_4(2\nu_3)$ than for $CH_4(\nu=0)$, again in support of this model.

The observed angular distributions also support the local-mode picture of stretch-excited methane reactivity. The measured laboratory-frame speed distributions for the $H+CH_4(\nu_3=1)\rightarrow CH_3(\nu_1=1)+H_2$ product channel, where the H atom reacts with an unstreched C–H oscilliator, are the same as that observed for $H+CH_4(\nu=0)\rightarrow CH_3(\nu=0)+H_2$ indicating that the vibration acts as a spectator and does not influence the dynamics.

Although Wu *et al.*[10] recently reported a full-dimensional quantum dynamics calculation of the thermal rate constant for $H+CH_4$, such calculations remain quite challenging for many other quantities of interest. As a result, much effort has been expended to determine which degrees of freedom are most important to include in models of reduced dimensionality. The current experiments allow us to make some observations relevant to this question. First, for the reaction of stretch-excited methane, it appears that a local-mode description of the CH_4 vibration is useful and suggests that the methane molecule need not be considered in its full dimensionality. On the other hand, we observe excitation of the stretching and bending modes in the methyl radical products, suggesting that in order to describe accurately the system these modes must be included in a description of the dynamics.

B. Reaction-path analysis

Insight into this reaction can also be obtained by examining the evolution of the normal modes of the CH_5 system as it progresses from reactants to products along the minimum-energy path. This method has its origins in the vibrationally adiabatic formulation of transition-state theory.[63,64] Assuming that the reaction coordinate can be separated from the other motions of the system and that the quantum numbers of the orthogonal modes do not change when motion along the reaction coordinate is slow, the reaction coordinate is the minimum-energy path (MEP) that connects reactants and products and is often parametrized as a function of s, the arclength along the reaction path. The energy of the vibrationally adiabatic potential curve is

$$V_a^g(n,s) = V_{\mathrm{MEP}}(s) + \varepsilon_{\mathrm{int}}^g(n,s), \tag{10}$$

where n is the quantum number of the generalized normal mode and $\varepsilon_{\mathrm{int}}^g(n,s)$ is the energy of the normal mode n when all other modes are in their ground state. In the reactant and product valleys, i.e., for $s=-\infty$ and $s=+\infty$, the generalized normal mode n correlates to a specific reagent and product normal mode. In this formalism, the coupling[65] between two modes m and m' is given by the coupling constant $B_{m,m'}(s)$ and the coupling of a given mode to the reaction coordinate F is given by $B_{m,F}(s)$. The reaction-path curvature for a polyatomic reaction[65] $\kappa(s)$ is given by the sum

$$\kappa(s) = \left\{ \sum_k [B_{k,F}(s)]^2 \right\}^{1/2} \tag{11}$$

and regions of large reaction-path curvature are known to promote vibrational nonadiabaticity. Calculations of the above-mentioned quantities have been performed for the new analytical potential-energy surface of Espinosa-Garcia,[23] which is based on the older surfaces of Steckler *et al.*[21] and Jordan and Gilbert.[20]

The CH_4 antisymmetric stretch ν_3 in the purely adiabatic case is a spectator mode, i.e., the frequency of this mode changes little along the reaction coordinate, which might indicate it is ineffective at promoting reaction. But this prediction is at odds with the result from our current experiments. The triply degenerate $CH_4(\nu_3)$ mode evolves into the $CH_3(\nu_1)$ and doubly degenerate $CH_3(\nu_3)$ modes; therefore, both of these modes should be excited in the products. The current experiments observe that a large fraction of the CH_3 products is excited into the symmetric stretch ν_1. Assuming that these products originate from the adiabatic channel, CH_3 products should also be excited into the antisymmetric stretch ν_3; however, this vibrational band has not been observed previously in the CH_3 $3p_z-X(2+1)$ REMPI spectra and only recently in the CD_3 $3p_z-X(2+1)$ REMPI spectra.[66] This may account for its absence in this work. In addition to the adiabatic product channel leading to $CH_3(\nu_1)$, we observe the nonadiabatic channels that lead to ground-state and umbrella bending excited CH_3. These results indicate that significant coupling occurs between the $CH_4(\nu_3)$ mode and the reaction coordinate or another reactive mode before the transition state.

These calculations of the reaction-path curvature indeed show two maxima, one on the reactant side, which is attributed mostly to the coupling of the reaction coordinate and the symmetric stretching mode, and one on the product side, which is attributed mostly to the coupling of the reaction coordinate to the H_2 stretching mode and a small contribution from the CH_3 bending mode. This also suggests, as above, that the $CH_4(\nu_3)$ mode is not reactive, but a region of large $\kappa(s)$ exists before the transition state. Therefore, energy may be partitioned into these modes, and the reaction path may be better described by the partial-reaction-path adiabaticity approach of Garrett *et al.*,[67] which to our knowledge has not been done for this system. While many features of the current experiments are suggested by the adiabatic corre-

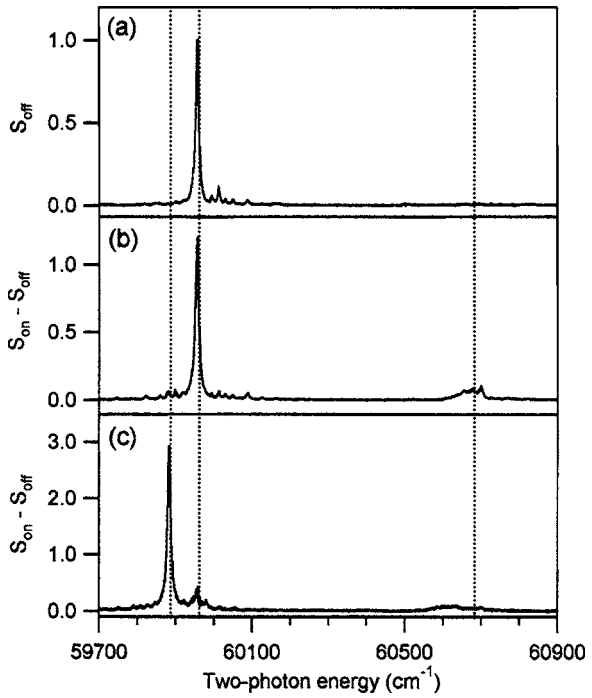

FIG. 7. Product $CH_3(2+1)3p_z \leftarrow X$ REMPI spectra for the reactions: (a) $Cl+CH_4(\nu=0)$, (b) $Cl+CH_4(\nu_3=1)$, and (c) $Cl+CH_4(\nu_3=2)$ at a center-of-mass collision energy of $E_{coll}=0.16$ eV. Reading from left to right, the positions of the 1_1^1 (C–H stretch), 0_0^0 (ground state), and 2_1^1 (umbrella bending mode) bands are marked by the vertical dotted lines. (a) displays the signal when the IR laser is off (S_{off}); (b) displays the difference $S_{on}-S_{off}$ obtained while the IR laser pumps the $\nu_3=1$, $F_2 \leftarrow A_1$, Q branch; and (c) displays the difference $S_{on}-S_{off}$ obtained while the IR laser pumps the $\nu_3=2$, $F_2 \leftarrow A_1$, Q branch.

lations, much remains unclear. We conclude that a more sophisticated model is necessary to explain the current experimental findings.

C. Comparing the reactions of Cl and H with stretch-excited methane

We compare the reactions of Cl and H with $CH_4(\nu_3=0,1,2)$ and propose a simple model to account for the observed differences. Figure 7 shows the CH_3 REMPI spectra obtained previously[38,40] for

$$Cl + CH_4(\nu = 0) \rightarrow CH_3 + HCl,$$

$$Cl + CH_4(\nu_3 = 1) \rightarrow CH_3 + HCl,$$

$$Cl + CH_4(\nu_3 = 2) \rightarrow CH_3 + HCl$$

at $E_{coll}=0.16$ eV. Figures 3 and 7 illustrate several similarities and differences between these two reactions. First, the ground-state reactions both produce predominantly ground-state CH_3 with the propensity for forming $CH_3(\nu_2)$ being larger for the H-atom reaction. This result is somewhat surprising considering that the data presented for $Cl+CH_4$ reaction were obtained with $E_{coll}=0.16$ eV whereas, the $H+CH_4$ reaction displayed in Fig. 3 was obtained for $E_{coll}=1.52$ eV. However, the data suggest that in both cases the abstraction reaction is local to one C–H bond and that the methyl radical product plays little role in the direct ground-state reaction. Second, excitation of the CH_4 $\nu_3=1$ vibration produces a dramatic change in the state distributions. The main CH_3 product channel from the Cl-atom reaction remains ground-state CH_3 and the state distribution is similar to the $Cl+CH_4(\nu=0)$ reaction. The dominant product channel for the H-atom reaction, on the other hand, is stretch-excited CH_3 with the ground-state CH_3 channel being smaller. The difference continues to manifest itself in the reactions of Cl and H with $CH_4(\nu_3=2)$. Overall, it appears that the Cl atom is more able to localize the vibration and transfer it to the "new" HCl bond, leaving the C–H spectator bonds in their vibrational ground state. The H atom is less effective at this endeavor and often the local C–H excitation in methane is transferred adiabatically to the methyl C–H stretching.

The explanation of this behavior is necessarily complex and could have many causes; however, we offer a few simple possibilities. We propose this observed behavior might arise because the H atom approaches the methane much more quickly than the Cl atom in these experiments. The vibrational period of $\nu_3=1$ is $\sim$11 fs. During this time, the distance between the H atom and the CH_4 in the center-of-mass frame decreases by $\sim$1.6 Å (for $E_{coll}=1.52$ eV), whereas the Cl-atom distance changes by only 0.2 Å in the same time interval (for $E_{coll}=0.16$ eV). Thus, the Cl atom might sample more vibrational periods during its interaction, allowing time for the vibration to be localized into the reactive bond and transferred to the HCl product. The Cl atom, when incident on the methane, is always able to localize at least one isolated C–H vibration into the bond that is broken. Thus, for the reaction $Cl+CH_4(\nu_3=1)$ the dominant product channel is ground-state CH_3, and for the reaction $Cl+CH_4(\nu_3=2)$ it is $CH_3(\nu_1=1)$. On occasion, the Cl atom is able to abstract both quanta of vibration from CH_4, even though it is initially localized in two different C–H oscillators, as illustrated by the small peak at the 0_0^0 transition! This means that the vibrational wave function is significantly perturbed by the approaching Cl atom in the transition state allowing flow of vibrational energy among the different modes into the reactive coordinate. This behavior might be regarded as intramolecular vibrational redistribution (IVR) in the transition-state region. The observed state distribution for the $H+CH_4(\nu_3=2)$ reaction is markedly different. It appears that the H atom is unable to localize the vibration into the reactive bond upon approach to the vibrationally excited CH_4 as effectively as the Cl atom. It is, of course, difficult to unravel the many factors at work. For example, we cannot exclude the possibility that the larger and more polarizable Cl atom is simply more able to localize the vibration caused by differences in the potential-energy surface, which by necessity plays a part in determining the relevant interaction region. In addition, it is the speed of the reagent and not the collision energy that matters in the above interaction time model. For the same collision energy, however, the H atom will always move $\sim$3.4 times as far as the Cl owing simply to the mass difference and, thus, our argument might be more general.

VI. SUMMARY

We have found that excitation of the antisymmetric stretching fundamental ($\nu_3=1$) and overtone ($\nu_3=2$) in meth-

ane enhances the $H+CH_4$ reaction cross section by a factor of 3.0 ± 1.5 for the former. Furthermore, stretch excitation of the CH_4 reagent leads to dramatic mode selectivity in the CH_3 product-state distributions. The observed CH_3 state distributions also suggest that the local-mode description of CH_4 is more appropriate for understanding the dynamics, even for the ν_3 fundamental. In this picture, H atoms incident on $CH_4|1000\rangle$ can either react with a stretched or unstretched C–H oscillator; the vibration is unable to localize during the time of interaction. The same picture holds for CH_4 excited to the $|1100\rangle$ state. Contrasting this with the reactions of Cl with the stretch-excited CH_4, we see that the Cl atom is better able to abstract vibrational energy from the methane and deposit it into the newly formed HCl bond. More theoretical and experimental works are clearly necessary to address the additional complexity associated with dynamics of an atom reacting with a polyatomic reagent.

ACKNOWLEDGMENTS

Two of the authors (H.A.B and J.P.C.) thank the National Science Foundation for graduate fellowships. One of the authors (H.A.B.) also acknowledges Stanford University for the award of a Stanford Graduate Fellowship. This material is based upon work supported by the National Science Foundation under Grant No. 0242103.

[1] R. L. Miller, A. G. Suits, P. L. Houston, R. Toumi, J. A. Mack, and A. M. Wodtke, Science **265**, 1831 (1994).
[2] H. Teitelbaum, P. J. S. B. Caridade, and J. C. Varandas, J. Chem. Phys. **120**, 10483 (2004).
[3] R. D. Levine, Combust. Flame **78**, 5 (1989).
[4] R. Zellner, in *Combustion Chemistry*, edited by J. Gardner (Springer, New York, 1984), p. 127.
[5] J. C. Polanyi, Acc. Chem. Res. **5**, 161 (1972).
[6] J. Warnatz, in *Combustion Chemistry*, edited by J. Gardiner (Springer, New York, 1984), p. 197.
[7] S. C. Althorpe and D. C. Clary, Annu. Rev. Phys. Chem. **54**, 493 (2003).
[8] J. M. Bowman, Theor. Chem. Acc. **108**, 125 (2002).
[9] F. Huarte-Larranaga and U. Manthe, J. Chem. Phys. **113**, 5115 (2000).
[10] T. Wu, H. J. Werner, and U. Manthe, Science **306**, 2227 (2004).
[11] S. Chapman and D. L. Bunker, J. Chem. Phys. **62**, 2890 (1975).
[12] T. Takayanagi, J. Chem. Phys. **104**, 2237 (1996).
[13] H.-G. Yu and G. Nyman, J. Chem. Phys. **111**, 3508 (1999).
[14] D. Wang and J. M. Bowman, J. Chem. Phys. **115**, 2055 (2001).
[15] D. Wang, J. Chem. Phys. **117**, 9806 (2002).
[16] M. Wang and J. Z. H. Zhang, J. Chem. Phys. **116**, 6497 (2002).
[17] M. Yang, D. H. Zhang, and S.-Y. Lee, J. Chem. Phys. **117**, 9539 (2002).
[18] Q. Cui, X. He, M.-L. Wang, and J. Z. H. Zhang, J. Chem. Phys. **119**, 9455 (2003).
[19] B. Kerkeni and D. C. Clary, J. Chem. Phys. **120**, 2308 (2004).
[20] M. J. T. Jordan and R. G. Gilbert, J. Chem. Phys. **102**, 5669 (1994).
[21] R. Steckler, K. J. Dykema, F. B. Brown, G. C. Hancock, D. G. Truhlar, and T. Valencich, J. Chem. Phys. **87**, 7024 (1987).
[22] Z. Konkoli, E. Kraka, and D. Cremer, J. Phys. Chem. A **101**, 1742 (1997).
[23] J. Espinosa-Garcia, J. Chem. Phys. **116**, 10664 (2002).
[24] D. L. Baulch, C. J. Cobos, R. A. Cox *et al.*, J. Phys. Chem. Ref. Data **21**, 411 (1992).
[25] M. J. Rabinowitz, J. W. Sutherland, P. M. Patterson, and B. R. Klemm, J. Phys. Chem. **95**, 674 (1991).
[26] P. M. Marquaire, A. G. Dastidar, K. C. Manthorne, and P. D. Pacey, Can. J. Chem. **72**, 600 (1994).
[27] M. G. Bryukov, I. R. Slagle, and V. D. Knyazev, J. Phys. Chem. A **105**, 3107 (2001).
[28] J. Sutherland, M. Su, and J. Michael, Int. J. Chem. Kinet. **33**, 669 (2001).
[29] G. Germann, Y. Huh, and J. Valentini, J. Chem. Phys. **96**, 1957 (1992).
[30] J. P. Camden, H. A. Bechtel, and R. N. Zare, Angew. Chem., Int. Ed. **42**, 5227 (2003).
[31] W. R. Simpson, A. J. Orr-Ewing, and R. N. Zare, Chem. Phys. Lett. **212**, 163 (1993).
[32] W. R. Simpson, A. J. Orr-Ewing, T. P. Rakitzis, S. A. Kandel, and R. N. Zare, J. Chem. Phys. **103**, 7299 (1995).
[33] W. R. Simpson, T. P. Rakitzis, S. A. Kandel, A. J. Orr-Ewing, and R. N. Zare, J. Chem. Phys. **103**, 7313 (1995).
[34] W. R. Simpson, T. P. Rakitzis, S. A. Kandel, T. Levon, and R. N. Zare, J. Phys. Chem. **100**, 7938 (1996).
[35] A. J. Orr-Ewing, W. R. Simpson, T. P. Rakitzis, S. A. Kandel, and R. N. Zare, J. Chem. Phys. **106**, 5961 (1997).
[36] S. A. Kandel and R. N. Zare, J. Chem. Phys. **109**, 9719 (1998).
[37] Z. H. Kim, H. A. Bechtel, and R. N. Zare, J. Am. Chem. Soc. **123**, 12714 (2001).
[38] Z. H. Kim, H. A. Bechtel, and R. N. Zare, J. Chem. Phys. **117**, 3232 (2002).
[39] H. A. Bechtel, Z. H. Kim, J. P. Camden, and R. N. Zare **120**, 791 (2004).
[40] H. A. Bechtel, J. P. Camden, D. J. A. Brown, and R. N. Zare, J. Chem. Phys. **120**, 5096 (2004).
[41] Z. H. Kim, H. A. Bechtel, J. P. Camden, and R. N. Zare, J. Chem. Phys. **122**, 084303 (2005).
[42] H. A. Bechtel, J. P. Camden, D. J. A. Brown, R. M. Martin, R. N. Zare, and K. Vodopyanov, Angew. Chem., Int. Ed. **44**, 2382 (2005).
[43] S. Yoon, S. Henton, A. N. Zivkovic, and F. F. Crim, J. Chem. Phys. **116**, 10744 (2002).
[44] S. Yoon, R. J. Holiday, and F. F. Crim, J. Chem. Phys. **119**, 4755 (2003).
[45] S. Yoon, R. J. Holiday, E. L. Sibert, and F. F. Crim, J. Chem. Phys. **119**, 9568 (2003).
[46] L. B. F. Juurlink, P. R. Mccabe, R. R. Smith, C. L. Dicologero, and A. L. Utz, Phys. Rev. Lett. **83**, 868 (1999).
[47] M. P. Schmid, P. Maroni, R. D. Beck, and T. R. Rizzo, J. Chem. Phys. **117**, 8603 (2002).
[48] R. D. Beck, P. Maroni, D. C. Papageorgopoulos, T. T. Dang, M. P. Schmid, and T. R. Rizzo, Science **302**, 98 (2003).
[49] R. R. Smith, D. R. Killelea, D. F. Delsesto, and A. L. Utz, Science **304**, 992 (2004).
[50] G. Herzberg, *Infrared and Raman Spectra of Polyatomic Molecules* (Van Nostrand, New York, 1945).
[51] E. Venuti, L. Halonen, and R. G. Della Valle, J. Chem. Phys. **110**, 7339 (1999).
[52] L. Halonen, J. Chem. Phys. **106**, 831 (1997).
[53] M. W. Chase, Jr., C. A. Davies, J. R. Downey, D. J. Frurip, R. A. Mcdonald, and A. N. Syverud, J. Phys. Chem. Ref. Data Suppl. **14**, 1 (1998).
[54] E. Kraka, J. Gauss, and D. Cremer, J. Chem. Phys. **99**, 5306 (1993).
[55] K. D. Dobbs and D. A. Dixon, J. Phys. Chem. **98**, 5290 (1994).
[56] P. L. Fast, M. L. Sanchez, and D. G. Truhlar, J. Chem. Phys. **111**, 2921 (1999).
[57] J. W. Hudgens, T. G. Digiuseppe, and M. C. Lin, J. Chem. Phys. **79**, 571 (1983).
[58] J. F. Black and I. Powis, J. Chem. Phys. **89**, 3986 (1988).
[59] J. Zhou, J. J. Lin, W. Shiu, S. C. Pu, and K. Liu, J. Chem. Phys. **119**, 2538 (2003).
[60] H. A. Bechtel, Z. H. Kim, J. P. Camden, and R. N. Zare, Mol. Phys. **103**, 1837 (2005).
[61] J. P. Camden, W. Hu, H. A. Bechtel *et al.*, J. Phys. Chem. A (in press).
[62] S. P. Walch, J. Chem. Phys. **72**, 4932 (1980).
[63] R. A. Marcus, J. Chem. Phys. **45**, 2630 (1966).
[64] D. G. Truhlar, J. Chem. Phys. **53**, 2041 (1970).
[65] W. H. Miller, N. C. Handy, and J. E. Adams, J. Chem. Phys. **72**, 99 (1980).
[66] B. Zhang, J. Zhang, and K. Liu, J. Chem. Phys. **122**, 104310 (2005).
[67] B. C. Garrett, D. G. Truhlar, J. M. Bowman, and A. F. Wagner, J. Phys. Chem. **90**, 4305 (1986).
[68] W. J. Van Der Zande, R. Zhang, R. N. Zare, K. G. Mckendrick, and J. J. Valentini, J. Phys. Chem. **95**, 8205 (1991).
[69] L. S. Rothman, A. Barbe, D. C. Benner *et al.*, J. Quant. Spectrosc. Radiat. Transf. **82**, 5 (2003).